Surface-Damage Mechanisms: from Nano- and Microcontacts to Wear of Materials

CHAPTER · DECEMBER 2006

DOI: 10.1007/978-3-540-36807-6_21

1 AUTHOR:

Rogerio Colaço
Instituto Superior Técnico, Lisbon, Portugal
133 PUBLICATIONS **1,348** CITATIONS

SEE PROFILE

NanoScience and Technology

E. Gnecco
E. Meyer (Eds.)

Fundamentals of Friction and Wear on the Nanoscale

Chapter 21
Surface-Damage Mechanisms:
from Nanoand Microcontacts to Wear of Materials
R. Colaço

Springer

21 Surface-Damage Mechanisms: from Nano- and Microcontacts to Wear of Materials

R. Colaço

Mat. Eng. Department, Instituto Superior Técnico Av. Rovisco Pais 1, 1049-001, Lisboa, Portugal rogerio.colaco@ist.utl.pt

21.1 Introduction

Most certainly life on Earth would be quite different from what we know without (or with different) tribologically related phenomena. For a few examples, one can think of the Earth's landscape, formed by a billion years of water and air erosion, the friction-controlled metastable equilibrium of geological faults and cracks, or simply by the way we (and all the things) move on the Earth's surface. Nevertheless, until the mid-1960s, not much attention had been paid to this science. Of course, some important exceptions are worth mentioning, but even the word "tribology" did not exist forty years ago. However, in 1966 a report made by a UK government committee presided by H.P. Jost, known as the *Jost Report*, found that a large waste of resources – estimated in 515 million pounds sterling per year (approximately 4% of the 1965 UK GNP) – occurred because of ignorance of surface-interaction phenomena [1]. Although friction, lubrication and wear had been studied for many years before (Leonardo da Vinci was among those who paid attention to tribological phenomena), the fact is that the Jost Report launched several R&D and education programs in tribology. The introduction in the lexicon of the word "tribology" – the science of rubbing – was one of the first consequences of this report.

Initially it was widely felt that the Jost Report greatly exaggerated the savings that might result from improved tribological expertise. Nevertheless, later it became clear that, on the contrary, the report underestimated the economical importance of tribology, since it paid small attention to wear, which happens to be, from an economical point of view, the most significant tribological phenomenon [2, 3].

In the last decades the experimental and theoretical research in tribology and, particularly, in the wear mechanisms of materials, have led to considerable advances. The generic "wear of materials" has been classified in different modes, in accordance with its type of occurrence and with its phenomenology (abrasion, adhesion, erosion, fretting, etc.); the damage mechanisms of rubbing surfaces have been identified (cutting, plowing, cracking, delamination, fatigue, oxidation, etc.) and mathematical models for wear, with more or less wider application ranges, have been developed.

These advances have certainly brought wear studies closer to a more predictive science, and important technological benefits have resulted from it. Some examples of technological advances closely related with the advances in tribological knowledge, and particularly in wear knowledge, are the hard disk drive technology and the development of digital light processing micromirrors (DLPMs) [4], the development of ceramic bearings [5] and the development of composite hardfacing materials for protective coatings [6]. Nevertheless, recent studies [7–9] still point to a non-negligible economical impact of tribologically related phenomena. In the US alone, recent estimations lead to values around US$ 8 billion per year spent in wear-related problems [10] and it is widely accpeted that at least 1% of the GNP of an industrialized country might be saved with minimal further investment in research [11, 12].

How to understand the maintenance of such high economical wastes in wear- and friction-related problems, in spite of the unquestionable increase in tribological knowledge in the last decades?

Most probably, many causes are the origin of this persistency over the years of the economical impact of tribological phenomena, particularly of wear. Perhaps the first factor to be considered is the fact that tribologically related problems are still not yet a main topic of concern for the common industrial engineer, who faces wear as an inevitability. This surely can be overcome with a stronger emphasis on tribology in undergraduate engineering programs. But, certainly, it also contributes to this persistency technologically related causes. On the one hand, in parallel with the growing development of tribological and surface engineering knowledge, there is also a growing demand to increase the production rates and efficiency of machines, tools and engineering components in general, which leads to higher working speeds and loads that result in more aggressive wear conditions. On the other hand, new systems and applications, in which tribological performance is a critical issue, have arisen in recent years. Some examples of this are the increasingly growing demands for higher storage densities and speeds in the magnetic disk drive technology, the growing interest in micro-/nano-electromechanical systems (MEMS and NEMS) and the demands for more wear-resistant biomedical implant materials, with increased *in-vivo* lifetimes and satisfying biocompatibility and bioactivity requirements. In these examples, new challenges for the tribologists arise, either because the variability of the contact conditions is rather complex (biomedical implant materials), or because of the reduction of the contact scales to the nanometric or even atomic ranges (electromagnetic microdevices).

In what concerns wear, a large number of recent studies have pointed to the need to understand deeper the atomic origins of wear [12] as well as to establish relations between macro-, micro- and nanowear phenomena [5], i. e. bridging the gap between observation scales.

From the application point of view, nanowear studies are not only important because of the growing importance of disk storage and of micro- and

nanotechnologies, but also for the optimization of more common and conventional tribological systems in engineering components. In fact, since the pioneering work of Greenwood and Williamson [13], it is well known that the contact between nominally flat surfaces (the most frequent in engineering components) occurs between small surface asperities, whose contact areas can be only of a few tens of square nanometers or even smaller. The point being made is that, even in conventional engineering systems, the interactions at nanometric scales cannot be neglected.

With the advent of the atomic force microscope (AFM) [14], it became possible to study wear phenomena at very small scales and loads. The AFM tips can be used to simulate a sharp single asperity travelling over a surface [15, 16]. By using a stiff steel cantilever with a sharp diamond tip (or diamond-coated tip) mounted on its end, nanowear experiments at high loads in hard materials can also be made [17–21]. AFMs can be used to measure or monitor, at very fine scales, the damage and/or topographical changes in surfaces after local rubbing (e. g. [22–24]) or to measure the work of adhesion between the surface and the single asperity simulated by the tip (e. g. [25,26]). As a consequence, the appearance of this instrument has opened a wide new field of research for tribologists, enabling entrance to the study of wear and damage mechanisms at the scales that were not acessible before.

This possibility of going to smaller and smaller scales in wear studies has raised a number of new questions, such as:

- what are the (or, are there) phenomenological thresholds between nanowear, microwear and macrowear?
- are the classical wear equations valid for rubbing at nanoscale, or are new ones needed for nanowear?

Generally speaking, these questions can be summarized in the general form "is the *scale* a characteristic of the tribological system that influences its response (such as speed, load, atmosphere, etc.) or, on the contrary, is the phenomenology kept if the tribological system is (homothetically) scaled down?"

Results obtained up to now are still scarce and progress still needs to be made, both from the experimental and theoretical points of view. There are not only scale gaps between "conventional" wear and nanowear, but also gaps between theory and experimental results on going to micro- and nanomechanical phenomena in general. As an example, there is clearly a need for the development of a micrometer level continuum theory, enabling a link from the macroscopic fracture process to the atomistic one to be made [27]. In fact, according to conventional plasticity theories, which are length-scale independent, the maximum stress level that can be achieved at a crack tip is not larger than 4–5 times the tensile yield stress of the material [28]. However, experimental studies show that the stress level needed to produce atomic decohesion in Nb-sapphire crystals can be up to 10 times its tensile yield stress [29]. This incompatibility between macroscopic fracture theories and

atomistic fracture results is apparently due to factors that become relevant at atomistic scales but that are not included in conventional plasticity theories.

This chapter aims to give a brief overview of the state-of-the-art in atomic, nano- and microwear knowledge.

21.2 The Nature of Solid Surfaces

The term "surface" can be understood as the transition region of a material to its environment [30], and this term will be used from now on with the more strict meaning of "solid surface".

From the tribological point of view, surface properties are a key factor for the performance of any moving component since, in contacting rubbing pieces, the work is dissipated in the surface and subsurface region. An "engineering surface" can be quite different from an ideal atomically smooth surface in vacuum conditions, whose equilibrium structure can be described, for instance, by the TLK (terrace, ledge, kink) model [31]. Two important differences should be considered between an engineering surface and a TLK surface. The first is the fact that, in the former case, the transition between the bulk properties and the environment is not as sharp as in the latter. The second is the fact that engineering surfaces have topographical features that can be several orders of magnitude larger than the atomic terrace and ledge scales. The tribological performance of an engineering component is therefore strongly dependent on the physical, chemical and mechanical properties of the surface (and by the gradients of these properties) and on the surface topography. Some aspects of these two topics will be briefly discussed next.

21.2.1 Surface Constitution

Solid surfaces in general can present several layers, with properties that can be quite different from the bulk ones. As a consequence, a solid surface is a portion of material that can present a rather complex structure and properties, which, in part depend on the surface preparation method, the nature of the solid and the interactions between the surface and environment (e. g. [11]).

Usually, in mechanically machined, ground or polished surfaces, there is a layer of deformed material (formed during the surface-preparation process). In metals and metallic alloys, this deformed zone usually is work hardened and can present a hardness higher than that of the bulk (see point 4). Bowden, Moore and Tabor were the first to observe clearly this deformed zone, by using taper-section optical microscopy [32].

On the top of this deformed layer sometimes is referred the presence of a smeared layer with an amorphous structure, whose thickness is a few nanometers, the so-called Beilby layer [33]. The Beilby layer is supposed to be produced by localized melting and surface flow during the mechanical surface-preparation process. However, its existence is indeed quite controversial [34],

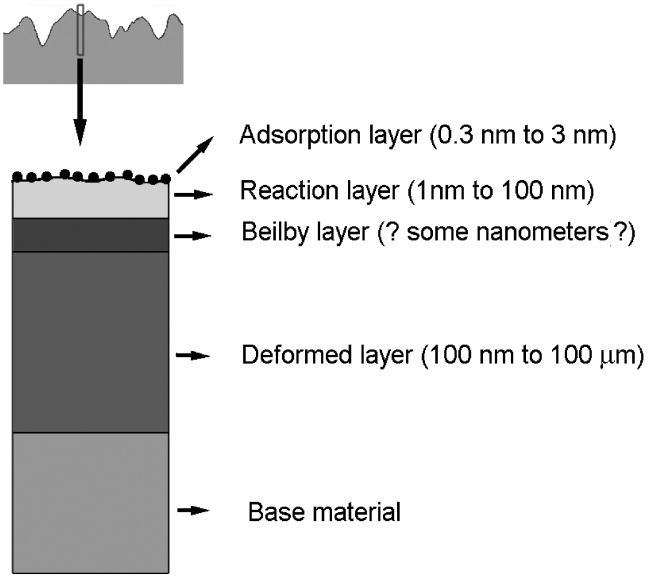

Fig. 21.1. Schematic view of a cross section in an engineering surface

and the attempts to characterize this layer by fast electron scattering [35] or by transmission electron microscopy [36] have never been conclusive.

Most surfaces are chemically reactive and form native surface oxide layers in air, or other reaction layers depending on the environment (nitrides, sulfides, chlorides, etc.). Besides these native films, adsorbed layers of molecules present in the environment (water, gaseous molecules, organic molecules, etc.) can also appear at the surface.

The presence of all these regions (schematically represented in Fig. 21.1), with their different properties, influences the tribological response of the material. Moreover, if the interaction scale of the damage during contact and rubbing changes between these regions, alterations in the wear response of the material can occur.

21.2.2 Surface Topography

Surfaces are rough. Even the most highly polished component has irregularities (asperities) significantly larger than the atomic scale. Figure 21.2 shows an AFM topographic profile (tapping mode) of a finely polished metallic surface (mirror-like finishing). The irregularities, or deviations from the nominal ideal flat surface, form the surface topography. The surface topography can show different features (such as flaws, pores, waviness, etc.). However the contact mechanics of solids depends essentially on the shorter-wavelength fluctuations [13, 37–39], the so-called roughness. Roughness also influences the dynamics (and vibrational modes) of the contact region of rubbing (or

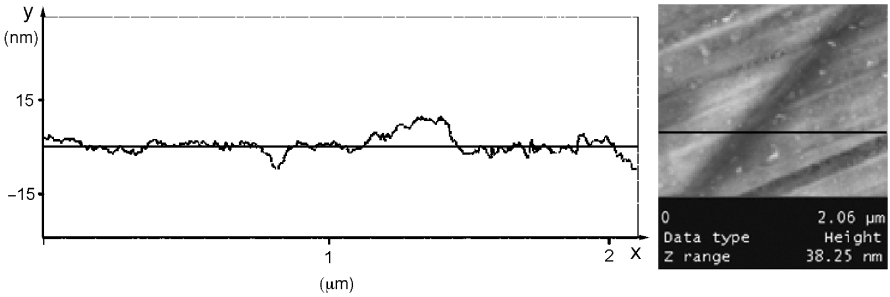

Fig. 21.2. AFM topographic profile of a mirror-like metallic surface, obtained by fine mechanical polishing with a suspension of 1 μm diamond particles

near-rubbing) sliding bodies (such as hard disk drive sliders) [40] and, of course, the wear response of the materials [41].

The surface roughness has a fractal nature, in the sense that it is formed of a large number of length scales superimposed on each other [42]. A wide number of roughness parameters and parametric functions can be used to describe and quantify surface roughness (a rather exhaustive presentation can be found in [39]). The most commonly used are roughness amplitude parameters (vertical descriptors), such as the average roughness, R_a, and the average maximum roughness, R_z, defined as:

$$R_\mathrm{a} = \frac{\int_0^{l_\mathrm{m}} |y| \, \mathrm{d}x}{l_\mathrm{m}} \tag{21.1}$$

in which l_m is the profile length, and $y(x)$ is the profile function in an axis whose origin is at the centerline of the profile (Fig. 21.2), and:

$$R_\mathrm{z} = \frac{1}{5} \sum_{i=1}^{5} y_i \tag{21.2}$$

with y_i being the maximum distance peak to valley in the i^{th} interval of the profile.

21.2.3 Topographic Mechanisms of Wear

Experience shows that, in general, smoother surfaces in rubbing contact exhibit lower wear than rougher ones, either in dry or lubricated contact conditions, and that the running-in period also decreases with increasing smoothness of surfaces [41, 43, 44].

An explanation for this behavior can be found in the early work of Greenwood and Williamson [13], on the contact mechanics of rough surfaces. The

basic idea of the GW model is that, since contact of rough surfaces occurs between the small asperities of opposing surfaces, the real area of contact, A_{R}, is different from the apparent area of contact, A_{N}. According to the GW model, A_{R} is independent of A_{N} and the ratio $A_{\mathrm{R}}/A_{\mathrm{N}} = f$ can be rather small (typically between 10^{-5} and 10^{-1}).

Since the height of the asperities is not uniform (see Fig. 21.2), when the surface is submitted to a normal load, F_{N}, the touching asperities are under different stresses, but it can be shown that the average stress in the touching asperities, $\langle\sigma\rangle$, is given by [45]:

$$\langle\sigma\rangle = \frac{\sigma_{\mathrm{N}}}{f} \tag{21.3}$$

in which $\sigma_{\mathrm{N}} = F_{\mathrm{N}}/A_{\mathrm{N}}$ is the normal (compressive) stress in the bulk material, in a plane parallel to the surface.

Equation (21.3) shows that even small elastic compressive stresses in the bulk can lead to high average stresses in the contact spots of the surfaces, since f can be rather small. Moreover, some of the asperities (those of higher amplitude) may deform plastically, while the others (the smaller amplitude ones) can deform in the elastic regime [45].

Although Greenwood and Williamson did not discuss the mechanism of creation of a wear particle, they pointed out that wear is much more probable in touching plastic asperities than in elastic ones. They introduced a plasticity index, Ψ, given by:

$$\Psi = \frac{E^*}{H}\sqrt{\frac{R_{\mathrm{p}}}{\rho}} \tag{21.4}$$

R_{p} and ρ are topographical parameters: the standard deviation of the asperities height distribution function and the curvature tip radius of the asperities, respectively ($R_{\mathrm{p}} \approx 1.25R_{\mathrm{a}}$, for a Gaussian height distribution [39]). E^* is the reduced Young modulus given by:

$$E^* = \left(\frac{1-\nu_1^2}{E_1} + \frac{1-\nu_2^2}{E_2}\right)^{-1} \tag{21.5}$$

with ν_i and E_i the Poisson's and Young's moduli, respectively, of each of the surfaces. H is the hardness of the softer surface (see Sects. 21.3 and 21.4 of this chapter for a more detailed discussion on the concept of hardness and hardness at different scales, respectively).

For $\Psi < 0.6$ the contacts are predominantly elastic and for $\Psi > 1$ the contacts are predominantly plastic. For intermediate values of the plasticity index, part of the asperities in contact are in the elastic regime and part in the plastic regime. The most interesting thing about Ψ is its independence on load: it only depends on mechanical properties of the surfaces (the ratio E^*/H is inversely proportional to a yield extension) and of their topographic characteristics.

Only very finely polished surfaces have plasticity indexes smaller than 0.6 [46]. As a consequence, most of the surfaces in contact rubbing engineering components have a "mirror-like" finishing, i. e. they are finely polished, in order to decrease Ψ, bringing the contacts as much as possible to the elastic regime. The idea is that this will result in a shorter running-in period and in a lower wear rate. It should be pointed out that, in a mirror-like surface, such as the one whose topographical profile is shown in Fig. 21.2, the maximum peak-to-valley amplitude is typically smaller than 50 nm and R_a is typically smaller than 10 nm. In such surfaces, very common in dry or lubricated moving engineering parts, the contacts will occur in nanometric scales, as schematically shown in Fig. 21.3. Even in 3-body abrasive wear situations, with free hard micrometric particles moving in-between well-polished surfaces, the wear damage and debris can be in the nanometric range. Figure 21.4 shows a scanning electron microscopy (SEM) image of the initial debris formed in a finely polished tempered tool steel surface, submitted to

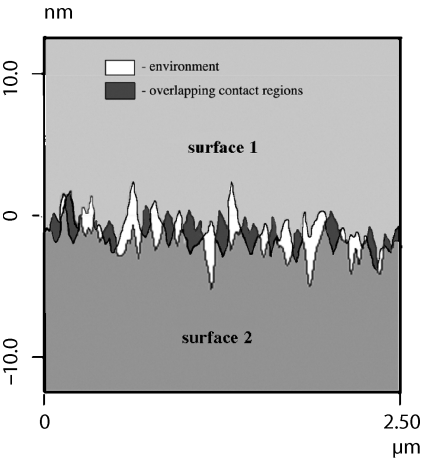

Fig. 21.3. Simulation of the contact regions of two surfaces with a roughness similar to that in Fig. 21.2

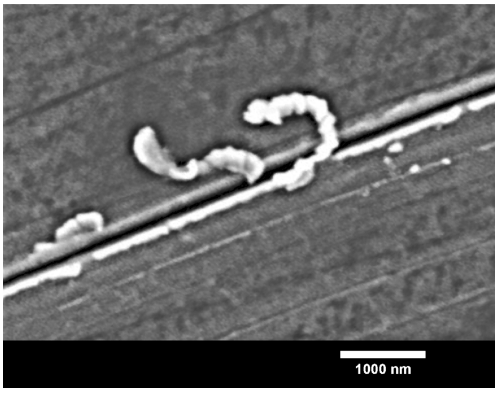

Fig. 21.4. Formation of the wear debris in a Cr tool steel when submitted to abrasion by hard 6 μm diamond particles. Typical wear coefficients obtained in such experiments are between 10^{-12} and 10^{-14} N/m^2 [47]

a common laboratorial ball-cratering abrasive wear test, with 6-μm diamond abrasive particles [47]. It can be observed that the typical dimensions of the scratch caused by the abrasive diamond particles (as well as that of the debris formed) are smaller than 150 nm.

The point being made is that, although up to now the studies concerning wear at nanometric scales have been performed mainly in electronically relevant materials (see Sect. 21.5 of this chapter), the wear mechanisms at this scale are certainly of a much wider relevance than that restricted to the wear of electronic and ultraprecision components.

21.3 Wear Theories

21.3.1 Classical Wear Theories

Probably, Holm [48] was the first to discuss the mechanisms of wear in his analysis on the relations between contact area and conductance. Later, Archard developed, based on some of Holm's ideas, a simple mathematical model for wear caused by adhesion between two opposing asperities [49]. The Archard wear equation for plastic contacts (usually known simply as the "Archard equation") is similar to that proposed by Holm, but Archard replaced the Holm's concept of "removal of atoms" by the concept of "removal of wear particles". So, in fact, the first model for wear was an atomic wear model.

In spite of its simplicity, the Archard model for "adhesive" wear is still widely used (sometimes outside of its developing context). The model considers two opposing asperities of materials with similar mechanical properties contacting during sliding. At some moment, the location of the two areas forming the contact is fully established (as shown in Fig. 21.5). A short time later the contact area is reduced to zero but, in addition, it is assumed that, at this moment, a new similar contact area has just been fully established somewhere in the surface. In each asperity contact, chemical interbonding and diffusion can lead to local sticking. The continuous relative motion can, thereof, result in a separation of the asperities at a surface different from

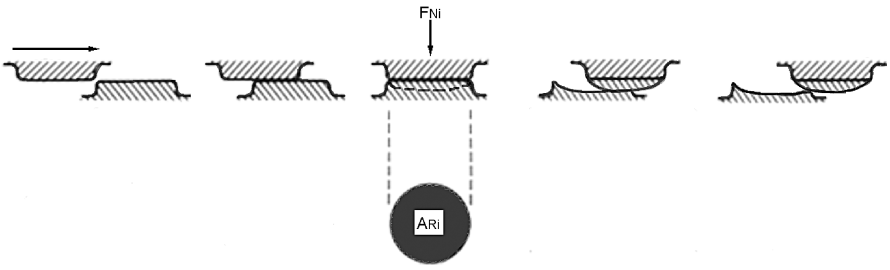

Fig. 21.5. Scheme of the Archard model for adhesive wear

the original one (Fig. 21.5), leading to surface damage and wear by material transfer.

The Archard model considers that the wear rate, Q_i, i. e. the volume of material transferred from one asperity to another per unit of sliding length, is simply proportional to the contact area when the contact is fully established, $A_{\mathrm{R}i}$:

$$Q_i = \frac{V_i}{L} = k_{\mathrm{ad}} A_{\mathrm{R}i} \tag{21.6}$$

Although it can be interpreted in various ways (e. g. see [50] for a detailed discussion), the factor, k_{ad}, is proportional to the probability that touching asperities adhere and originate mass transfer from one surface to another.

As previously discussed (point 2), the most probable wear mechanism is that the contacting asperities are plasticized and wear occurs by the removal of material lumps. If the asperities are fully plasticized, when submitted to a force $F_{\mathrm{N}i}$, than $A_{\mathrm{R}i}$ results directly from Tabor's definition of hardness [51]:

$$A_{\mathrm{R}i} = \frac{F_{\mathrm{N}i}}{H} \tag{21.7}$$

with H the hardness of the material. From Eqs. (21.6) and (21.7) one can obtain:

$$Q_i = k_{\mathrm{ad}} \frac{F_{\mathrm{N}i}}{H} \tag{21.8}$$

Assuming that all the contacts are fully plasticized ($\Psi > 1$), the total wear rate is simply:

$$Q = \sum Q_i = \frac{k_{\mathrm{ad}}}{H} \sum F_{\mathrm{N}i} = k_{\mathrm{ad}} \frac{F_{\mathrm{N}}}{H} \tag{21.9}$$

Eq. (21.9) was deduced for fully plastic contact conditions but Archard proposed the more general relation:

$$Q_i \propto F_{\mathrm{N}}^n \tag{21.10}$$

with $n = 0.6, 0.75, 0.8$ or 1, depending on whether the contacts are elastic or plastic and on whether the wear particle transferred is layer-like or lumpy-like (e. g. Eq. (21.9) is the particular case of Eq. (21.10) with $n = 1$, which stands for plastic contacts and lumpy-like transfer).

However, the subsequent work of Greenwood and Williamson [13] showed that, for multiasperity contacts, A_{R} is always directly proportional to F_{N}, independently of the contacts being elastic or plastic. Assuming this, the direct proportionality between wear rate and load stands not only for fully plastic contact conditions. In this way, a more general form of Equation (9) is simply:

$$Q = k_{\mathrm{ad}} \frac{F_{\mathrm{N}}}{\phi} \tag{21.11}$$

ϕ is the hardness, H, if the contacts are fully plasticized, or an "elastic contact hardness" if the contacts are in the elastic regime. For Gaussian surface

profiles this elastic contact hardness is given by [13]:

$$\phi = 0.25E^* \sqrt{\frac{R_\mathrm{d}}{\rho}} \tag{21.12}$$

A different situation is that of contacting surfaces with very different chemical and mechanical properties. In particular, if the hardness of one material is higher than that of the other (typically $H_1 > 1.2H_2$ as a rule of thumb [10]), the harder asperities will indent the softer material. The relative motion will lead to the formation of a groove (as shown in Fig. 21.6), resulting in "abrasive" wear of the softer material. This type of wear damage is not caused by adhesion, but rather by mechanical deformation and cutting. Therefore, the Archard model is not valid for "abrasive" wear.

Rabinowicz [52] proposed a different approach for abrasive wear. Assuming a conical asperity of the harder surface, infinitely rigid, that, when submitted to a load F_N indents the softer surface. After the softer surface become fully plasticized (Fig. 21.6), the equilibrium condition in the load application axis is given by:

$$F_\mathrm{N} = HA_\mathrm{R} = H\frac{\pi r^2}{2} = H\frac{\pi}{2}tg^2\theta h^2 \tag{21.13}$$

with r, h and θ defined in Fig. 21.6.

If all the material displaced from the groove is removed, than the worn volume, V, is given by:

$$V = Lrh = Lh^2tg\theta \tag{21.14}$$

From Eqs. (21.13) and (21.14) one can obtain,

$$Q = \frac{V}{L} = k_\mathrm{ab}\frac{F_\mathrm{N}}{H} \tag{21.15}$$

with $k_\mathrm{ab} = 2/(\pi tg\theta)$.

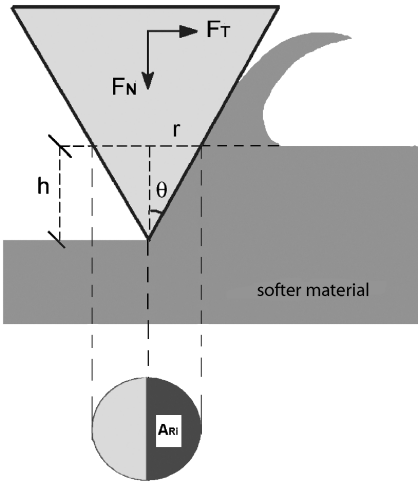

Fig. 21.6. Scheme of the Rabinowicz model for abrasive wear

By comparing Eqs. (21.9), (21.11) and (21.15), it can be concluded that the Rabinowicz model for abrasive wear is formally identical to Archard's model for adhesive wear. Moreover, the equations are identical to those obtained by Holm for "atomic wear" [48].

Apparently, this can be a quite surprising result since the phenomenology of each type of wear is different. But, in fact, all these approaches are based on the same basic idea: the worn volume is directly proportional to the real contact area between the tribological pair. This real contact area is proportional to the ratio F_N/H, for fully plastic contacts, or to the ratio F_N/ϕ (with ϕ defined in Eq. (21.12)), for GW Gaussian multiple elastic contacts.

Therefore, it seams that a more general equation for wear due to the relative motion of contacting surfaces can simply be:

$$Q = k_{tot} A_R \tag{21.16}$$

with k_{tot} an additive wear coefficient, with contributions of the active wear mechanisms in a given situation. Equation (21.16) applies in all the cases for which the wear rate is proportional to the contact area (there are some exceptions, e. g., the case of wear of brittle materials [53]).

21.3.2 Atomic Wear Theories

From the simple formulation given by Eq. (21.16), there is no discontinuity between wear occurring at atomic/nanometric scales and at larger ones: if the real contact area decreases to nanometric scales the wear rate decreases proportionally (as already mentioned, Holm's "removal of atoms" theory [48] led to an equivalent equation). Of course, from the predictive point of view, Eq. (21.16) is of limited helpfulness, since there is an uncertainty related with k_{tot}. The wear coefficient, k_{tot}, by depending on the active wear mechanisms, will surely also be scale dependent.

As the contact scale decreases to near-atomic lengths, the wear mechanisms involving extensive plastic deformation and crack propagation, such as grooving, delamination or fatigue, cannot be predominant if only a few atomic layers are involved in the contact. Molecular dynamics simulations, in contact scales involving a few atomic layers, show that at this small length scale, wear is essentially controlled by the dragging of atoms from their initial positions [54, 55].

Bassani and D'Acunto [56] developed a theoretical approach to the atomic dragging between a flat surface and an AFM tip under adhesive contact conditions. The approach used is based in a double-well potential model, in which the wear volume is quantified in terms of the atomic transition between the two well minima. According to this model, the total wear volume per unit time, V_t (i. e. the total volume of the atoms jumping from the flat surface to the tip surface in unit time) is given by:

$$V_t = n\omega V_{at} \tag{21.17}$$

where n is the initial atomic population, ω is the transition rate, and V_{at}, the atomic debris volume (note that this atomic debris is not necessarily an atom, since it can be an ionic pair or a polyatomic molecule, for instance). The transition rate between wells is given by an Arrhenius law:

$$\omega = \omega_{\mathrm{o}} \exp\left(-\frac{\Delta U}{kT}\right) \tag{21.18}$$

in which ΔU is the height of the energy barrier between the two well minima.

Later, D'Acunto [57,58] extended the model to the quantification of wear mechanisms at the nanoscale. It was proposed that the atomic wear rate (i. e. wear in which the active mechanisms are dragging of atoms (or ionic pairs) from their original positions) could be separated into two basic mechanisms: adhesion and abrasion. At this point it should be emphasized that the concept of "adhesive" and "abrasive" wear at the atomic scale does not have exactly the same meaning as defined previously, when the Archard and Rabinowicz models were presented. At atomic scales, adhesive wear was used for the cases in which the vertical (Van der Waals) forces are predominant and the atoms transfer from one surface to another. Conversely, atomic abrasive wear was used for the case in which shear forces are predominant, leading to the dragging of atoms to further positions from the primitive ones (in this case, the atoms do not jump from one surface to another). Figure 21.7a and b illustrates schematically the atomic adhesive and abrasive wear concepts.

The wear volume per unit of time defined in Eq. (21.17) can be transformed in a wear rate by dividing by the scanning speed of the asperity / tip, V_{s}. By doing this, D'Acunto's model leads to the following expression for the

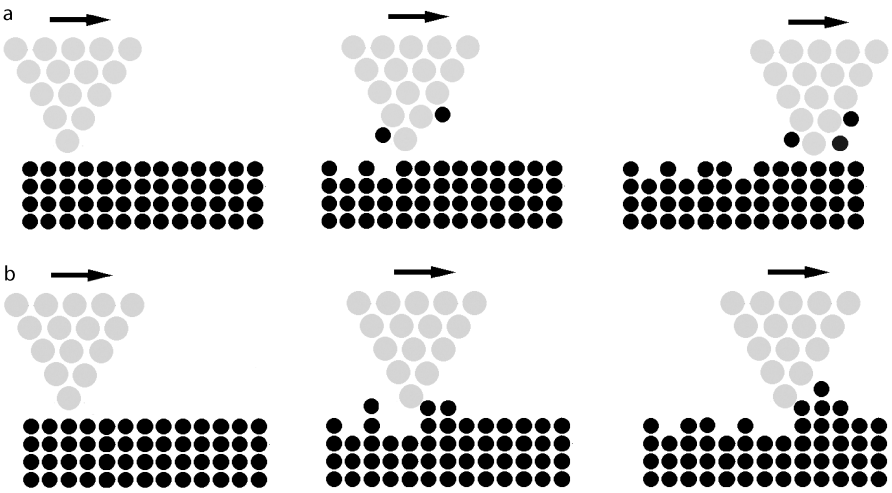

Fig. 21.7. Scheme of atomic adhesive wear (**a**) and atomic abrasive wear (**b**)

wear rate at the atomic scale:

$$Q = \frac{n\omega V_{\mathrm{at}}}{V_{\mathrm{s}}} \tag{21.19}$$

By noting that n can be given by $A_{\mathrm{R}}/A_{\mathrm{R}/n}$, with $A_{\mathrm{R}/n}$ the specific area per contact atom, Eq. (21.9) can be rewritten in the equivalent form:

$$Q = k_{\mathrm{at}} A_{\mathrm{R}} \tag{21.20}$$

with,

$$k_{\mathrm{at}} = \frac{\omega V_{\mathrm{at}}}{A_{\mathrm{R/n}} V_{\mathrm{s}}} \tag{21.21}$$

In spite of the formal similarity between Eq. (21.20) and Eq. (21.16), this result is different from what is obtained for bulk wear. According to theories for abrasive and adhesive wear at bulk scales (Eqs. (21.9) and (21.15), respectively), the wear rate is independent of the scanning speed, if the wear mechanism does not change within a certain range of speeds (e. g., see Lim and Ashby approach to sliding wear [59]). Therefore, an important result arising from this model, is that, atomic-scale wear is inversely proportional to the travelling speed of the counterbody. This is caused by the fact that, if speed increases, the interaction time for atom jumping decreases. Experimental observations for atomic wear of ionic crystals [23] do not show a significant velocity dependence of atomic wear as expected from the model. However, the experimental data and the velocity ranges tested are still scarce and further work is certainly necessary (in point 5 a more detailed overview of the experimental results, obtained up to now in nanoscale and atomic wear experiments, will be presented).

21.4 Hardness at Different Scales: is Smaller Harder?

Hardness is a measure of the yield stress of the material [51]. The appearance of this property in Archard and Rabinowicz wear models (Eqs. (21.9) and (21.15), respectively) is related to the fact that hardness measures the resistance of the asperities to the start of the dissipative plastic deformation processes, which can result in the formation of wear particles. Plastic deformation mechanisms are essentially related to the creation and movement of dislocations in metals and ceramics and chain reptation in polymers. As a consequence, if the interaction between body and slider is only of a few atomic layers, the deformation processes are inactive, and the nature of wear must be distinct, as discussed in point 3.2.

However, there is a length-scale range, from a few atomic layers to submicrometric lengths, in which, although the deformation mechanisms are already still active, the mechanical response of the material can be different

from its "bulk" mechanical response. In this (poorly defined) length range, the transition from "bulk wear" mechanisms to "atomic wear" mechanisms occurs. Changes in hardness with the indentation depth are particularly useful to identify this transition region, with the advantage that this property can be directly related to the wear behavior of the material.

In recent years there has been a growing interest in the use of molecular dynamics simulations (MD) methods to investigate nanoindentation [12]. Landman et al. [54], carried out one of the first MD simulations of a Ni tip indentating a gold surface. Subsequently, MD has been used in several studies of nanoindentation in different materials (e. g. [60–63]). Although, at present, atomistic methods allow for simulations of up to millions of atoms in time scales of microseconds, and provide information about the single-atom role in the contact [12], the length and time scales are still insufficient to provide more extensive links to experimental data [5]. Particularly, in the scale lengths of a few hundreds of nanometers there is a gap of understanding, since it is one too large scale for atomistic simulations and a too small scale for continuum mechanics theories to be still valid [64].

The fact is that, in this scale range of a few hundreds of nanometers, a large number of experimental works have shown that, in general, an increase of the hardness of the material occurs as compared with its bulk hardness, the so-called *indentation size effect* (ISE). ISE has been observed in a significant variety of metals, metallic alloys and ceramics: Cu [65, 66], Mo and W [67], Ag [68], Al and brass [69], Ni and Co [70], sapphire and MgO [71], TiO_2 and SnO_2 [72], LiF and NaCl [73], among others.

There are various explanations for the observed indentation size effect, including the sample preparation and test methods and the increasing perfection of the materials as the volume is reduced [71]. Of course, as mentioned in point 2.1, the constitution of the material changes on approaching the surface (Fig. 21.1). This, most certainly, will lead to different material properties, in particular to different hardness results, as the indenter crosses the different layers, schematically represented in Fig. 21.1. In particular, it has been observed that the deformed layer caused by the mechanical polishing of surfaces may contribute to the increase the hardness of metallic surfaces [66, 71]. Nevertheless, the ISE is still observed in electropolished samples and, in fact, the results strongly indicate that the ISE is an intrinsic material characteristic [74].

Conventional plasticity theories, which are based in continuous mechanics and, thus, do not involve a length-scale dependency, do not provide an explanation for the size dependency of hardness. Up to now, there are two theories that seem to offer the best explanation for the ISE: geometrically necessary dislocations (strain-gradient plasticity) [75] and surface free-energy effects [76, 77]. These two explanations for the indentation size effect will be briefly reviewed.

When a material is plastically deformed dislocations are generated, moved and stored. This storage causes the material to work-harden [78]. Disloca-

tions can be randomly distributed and stored, forming a network of defects in the crystalline structure of the material and, in this case, they are called statistically stored dislocations (STDs) [79]. In nonuniform deformation, dislocations are necessary for compatibility reasons and, in this case, they are called geometrically necessary dislocations (GNDs) [79, 80].

In the case of indentation experiments, the hypothesis is that plastic strain gradients surrounding the indentation are accommodated by the formation of these geometrically necessary dislocations. Since, in general, strain gradients are inversely proportional to the length scale over which plastic deformation occurs as the indentation depth decreases the density of GNDs must increase. This will lead to an increase of the hardness of the material [81, 82]. Based on these assumptions, Nix and Gao [75], proposed a model that relates the indentation size effect with the density of GNDs. The Nix–Gao model leads to a simple relation between the variation of the materials hardness caused by the GNDs, ΔH_{GND}, and the indentation depth, h [75]:

$$\Delta H_{\mathrm{GND}} = H_0 \left(\sqrt{1 + \frac{h^*}{h}} - 1 \right) \tag{21.22}$$

H_0 is the material hardness at an infinite depth (the "bulk hardness"). h^* is a characteristic length that depends on the shape of the indenter and on the tested material, given by:

$$h^* = \frac{3}{2} \frac{\tan^2 \theta}{b \rho_{\mathrm{s}}} \tag{21.23}$$

where b is the Burgers vector of the dislocations and ρ_{s} is the density of statistically stored dislocations. θ is the angle between the top surface of the material and the indenter.

Surface free-energy-related effects can also contribute to the increase of the hardness with decreasing scale, since the area to volume ratio increases as the scale decreases [76, 77]. According to Jager [77], surface free energy can have a non-negligible contribution to hardness if the three following conditions are simultaneously met: a) soft ductile samples with high SFE; b) sharp indenter geometries; c) shallow indentations.

Recently developed models accounting for the contribution of SFE to hardness lead to a relation of the type [76, 77]:

$$\Delta H_{\mathrm{SFE}} = \kappa \frac{E_{\mathrm{s}}}{h} \tag{21.24}$$

where ΔH_{SFE}, is the hardness variation with depth caused by SFE effects, E_{s} is the surface free energy, h the indentation depth, and κ a constant that depends on the geometry of the indenter (e. g., for a Veeco DNISP diamond AFM tip, $\kappa \approx 3.43$ [70]).

Assuming that both these effects (GNDs and SFE) are independent, and thus additive, it results from Eqs. (21.23) and (21.24), that a general equation

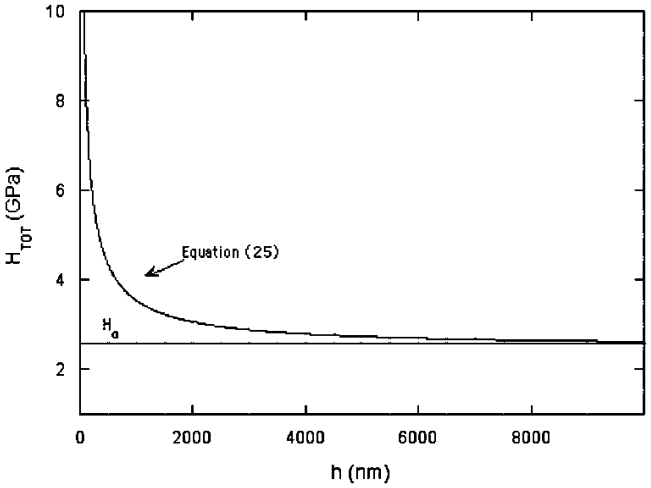

Fig. 21.8. Hardness variation with indentation depth according to Eq. (21.25). The plot was calculated with a set of values typical of a metallic alloy, e. g. a plain carbon steel: $H_0 = 2.5\,\mathrm{GPa}, E_\mathrm{s} = 2\,\mathrm{J/m^2}$ and $h^* = 1000\,\mathrm{nm}$ [75]). κ was taken as 3.43 [70]

for hardness as a function of indentation depth, accounting for both effects, has the form:

$$H_\mathrm{TOT} = H_0 + \Delta H_\mathrm{GND} + \Delta H_\mathrm{SFE} = H_0\sqrt{1 + \frac{h^*}{h}} + \kappa\frac{E_\mathrm{s}}{h} \qquad (21.25)$$

A typical plot of Eq. (21.25) is shown in Fig. 21.8. The plot was calculated with a set of values typical of a metallic alloy, e. g. a steel: $H_0 = 2.5\,\mathrm{GPa}, E_\mathrm{s} = 2\,\mathrm{J/m^2}$. h^* was taken as 1000 nm [75] and κ as 3.43 [70].

As can be observed, for indentation depths smaller than some thousands of nanometers, the combined effect of geometrically necessary dislocations and surface free energy can result in a non-negligible increase of the hardness. This increase can be particularly relevant in the submicrometric ranges. Therefore, both experimental and theoretical results obtained up to now seem to lead to the same conclusion: smaller tends to be harder, i. e. as the contact scale decreases to submicrometric ranges the resistance of the material to plastic deformation increases.

Our understanding of the theory of nanoindentation has certainly improved in recent years. However, many questions remain, such as strain rate and temperature dependence, dislocation nucleation and glide mechanisms [12]. Nanoindentation mechanics must certainly have an impact on the wear behavior of materials as the contact scale is reduced. There is certainly a need for comparative wear studies at micro- and (supra-atomic) nanometric scales. This will be an interesting research topic that, surely, will grow in the near future.

21.5 Nanoscale Wear Experiments

The development of atomic force microscopes [14], twenty years ago, has provided tribologists with a new tool that enables experiments from atomic scales to (almost) bulk ones. Up to now, an increasing number of studies has dealt with this topic but, as pointed out some years ago by Carpick and Salmeron [83], since this field is still in its infancy (may be in its preadolescence now), results so far are generally sporadic in scope and direction. Yet, a trend of growth is clearly perceptible, which will certainly continue in the future, due to the undeniable scientific and technological relevance of the field [84].

AFM experiments have shown that observable tip-induced wear in the sample (and also wear of the tip itself [20,85,86]) can occur when the AFM tip slides in contact with the sample, above some threshold load [83]. Tip-induced nanowear experiments have been performed (in UHV and environmental conditions) in a relatively large range of materials, such as thin films of AgBr and C_{60} deposited on NaCl [87], NaCl [88], KBr [23,89,90], PZTs [20], polymeric magnetic tapes [84], silicon [91, 92], SiO_2 [92], mica [93, 94], thermoplastic and thermoset polymers [95–97], among other materials. Fewer experiments have been performed with metals, possibly because, as pointed out by Gnecco et al. [89], metals are not the best candidates to study wear mechanisms by AFM, since the debris tend to accumulate on the tip, leading to a poor reproducibility of measurements. Still, some results on gold [98], MnZn ferrites [99], Cu [91] and Cr thin films [100] can be found in the literature.

One of the first in situ observations of the transition threshold to detectable wear in AFM experiments was made by Hu et al. [93]. The experiments were performed in mica, with silicon nitride probes, in air, water and ethanol environments. While monitoring the frictional forces, these authors observed that, once a certain critical load threshold was reached, the wear of mica (remotion of an atomic layer) was responsible for a transition from a linear relation between friction and load to a stochastic behavior (Fig. 21.9). The experiments showed that the wear of this layer of mica occurs both at high loads, in a single scan, or at lower loads, in multiple scans. This result strongly indicates that the load onset for atomic wear of mica has somehow a memory effect to the number of scans of the counterface slider. Hu et al. [93] suggested that, in the lower-load regime, point defects were accumulating during each scan. When the number of scans reaches a critical value, this accumulation will result in the formation of a small cluster (a nanodebris), resulting from the removal of one atomic layer. Recently, Helt and Bateas [101] were able to observe the nucleation of defects in muscovite mica under aqueous environments, prior to gross wear, confirming the nanowear mechanism proposed by Hu et al.

Gnecco et al. [23] have performed abrasive wear experiments at nanoscale on (001) KBr. They have shown that, under UHV conditions, the atomic-scale wear of KBr is due to the removal of single ion pairs. They have also shown

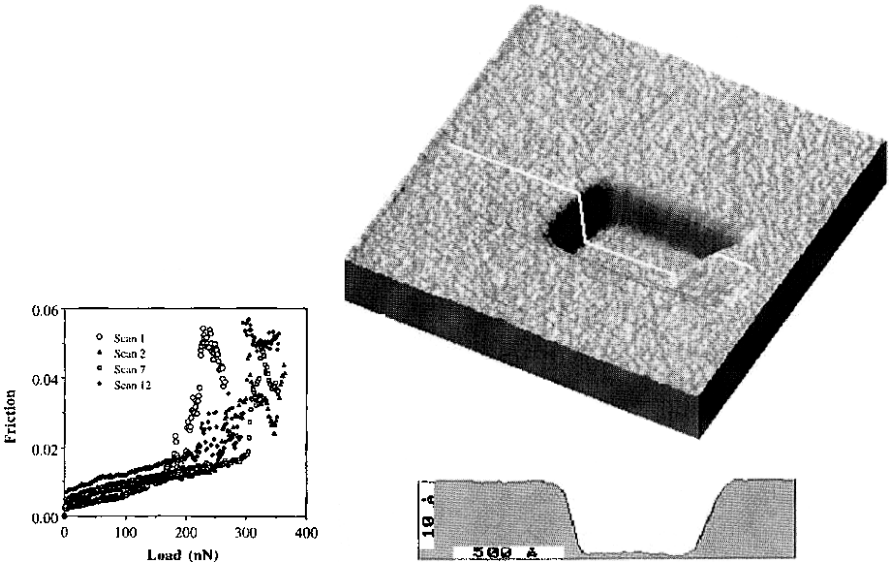

Fig. 21.9. Friction force (au) versus load in the high-load regime for multiple scans of a silicon nitride tip in contact with mica. Friction increases smoothly with load until wear occurs. At this time abnormal changes in the friction behavior are observed [93]

that the wear debris is reorganized in regular terraces with similar structure and orientation as in the unscratched surface. More recent experiments performed by the same group [90], also confirmed the cumulative nature of wear at atomic scales. In fact, they observe that, even at very low loads (between 1.7 and 30.1 nN) scratching of KBr with silicon probes in UHV conditions, always results in groove formation, after a sufficient number of scans is reached. Concomitantly, an irregular ripple formation in the periphery of the grooves was observed. This ripple-like structure appears after the onset of wear and has a periodicity that matches well with the scale length of the tip radii. In this way, the authors attributed the KBr wear mechanism at atomic scale to an accumulation in front of the tip of ionic pairs or small ion clusters. Ripple arises when the material transported by the tip increases friction and the tip jumps over it as the process restarts.

The experimental results obtained up to now seem to indicate that, in general, the precursor mechanism for atomic-scale wear is the formation of point defects that lead to the formation of small clusters. It is interesting to note that these observations match quite well with the theoretical double-well approach presented in Sect. 21.3.2. In fact, according to this model, in each interaction between surface and counterface atoms, there is a probability of atomic jumps to occur to the opposite surface (adhesion) or to another position in the same surface (abrasion). These jumps will result in the formation of point defects. Thus, both experimental and theoretical results seem to con-

firm that, in general, the formation of point defects in sliding contacts is the precursor mechanism for atomic wear. This mechanism is predominant in situations in which the contact loads are below the onset of plastic deformation or crack nucleation.

In a small, but relatively larger contact scale, Wang and Kato [102, 103] made a set of interesting wear experiments inside the chamber of an E-SEM (environmental scanning electron microscope). The experiments were performed with a pin-on-disk geometry in carbon nitride coatings and in bare Si(111). A diamond pin with a 10-μm curvature radius and a load range between 10 and 250 mN were used. One of the aims of the experiments was to observe the onset of wear from "no observable wear particles" to "wear-particle formation". This transition was defined when the formation of a cluster of worn particles, larger than 0.25 μm, could be confirmed by in situ E-SEM observation. The worn particles were described as "feather-like", for the mild wear regime, and "plate-like", for the higher wear regime.

Figure 21.10 summarizes the results obtained for the carbon nitride coatings. It can be observed that the transition from "no observable wear particles" to "wear-particle formation" depends on the load (as expected). However, the transition also occurs, in certain load conditions, when a critical number of cycles is reached. The authors have attributed this wear transition dependence of the number of cycles to a low-cycle fatigue wear mechanism [103]. However, and in spite of the higher loads used in Wang and Kato's experiments, it is worth mentioning the similarities with the observations for the nanowear onset of mica (Fig 21.9) [93].

As previously mentioned, when the load increases, resulting in higher depth interactions, other wear mechanisms become active. Also, the chemical

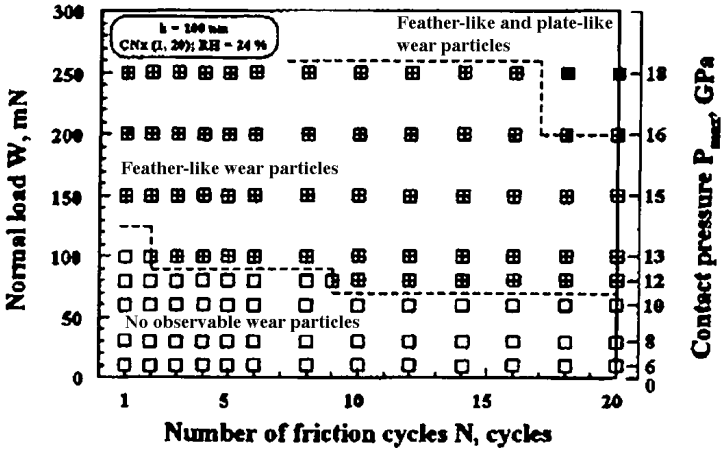

Fig. 21.10. Occurrence of wear particles of a carbon nitride coating, in terms of load and friction cycles, based on E-SEM observations [102]

Table 21.1. Wear coefficients for Si obtained in tests performed at different loads (after [91])

Material	Load	Test	Wear coefficient (as defined by Eq. (21.9) or (21.15))	Ref.
Si (100)	10 – 30 μN	Specimen-on-disk	10^{-5}	[104]
Si (100)	100 μN	AFM	10^{-1}	[105]
Si (111)	100 mN	Pin-on-disk in SEM	10^{-4}	[102]
Si	100 mN	Pin-on-disk	10^{-3}	[106]

and structural composition of the surface interlayers can change (Fig. 21.1). As a consequence, the wear response of the material can be quite different and, moreover, unpredictable, depending on the contact scale. For now, it seems that the only choice for tribologists is to carefully choose representative test conditions, in view of the application. The results obtained by Miyake et al. [19] for diamond and N^+-implanted diamond films clearly illustrate this point. These authors have observed that nanowear AFM tests, with loads in the range of μN, lead to the lowest wear resistance in N^+-implanted diamond films, as compared with diamond films. On the contrary, N^+-implanted films present the highest wear resistance in reciprocating wear tests, with loads in the range 0.098 to 4.9 N. This difference was attributed by the authors to the formation of a thin amorphous layer in the N^+-implanted samples (as observed by Raman spectroscopy), whose properties are relevant for AFM wear tests but not for the wear tests at higher loads.

Chung and Kim [91] presented a summary of the results obtained for low-load wear experiments, in materials for MEMS and ultraprecision electronic applications. The data was obtained by different authors, using low-load pin-on-disk and AFM tests in Si-based materials, carbon films and DLCs. The load ranges used changes from μN to mN. Table 21.1 shows the results for silicon, as reviewed by Chung and Kim. These results show that, although a general perception of the basic small-scale wear mechanisms starts to exist, extreme difficulties in quantifying wear still remain.

Clearly, advances can only be made if precise and reproducible experiments are available to test theoretical models [5]. Due to the complex nature of mass-dissipation phenomena, this goal is still to be achieved and, certainly, will continue to be a target for future endeavors.

21.6 Conclusions

In conclusion, one can say that there has been a great interest in submicrometric wear studies within the last 10 – 15 years. These studies cover different types of materials, different length scales (going from quasiatomic to quasi-

bulk ones) and different research objectives (from generic theoretical studies to well-focused application ones). Although the natural dispersion of results, caused by the great complexity of the phenomena involved, and to the youthful nature of the field, significant advances have been made in recent years.

The models and results obtained up to now suggest that, on approaching atomic scales, a division of mechanisms can be made between "atomic wear" and "bulk wear", i. e. wear involving atomic jumps and point-defect formation (the former) and wear involving plastic deformation and crack propagation (the latter).

For atomic wear, experimental results strongly suggest that there is threshold for detectable wear. This threshold is a load threshold but can also be a number of contact cycles threshold. This suggests a cumulative nature for atomic wear, which is in agreement with theoretical models.

For higher loads and higher contact interaction depths, plastic deformation and crack propagation mechanisms will be activated, and the wear can, in principle, be described by classical continuum-mechanics-based theories. However, it should be noted that there is a length scale interval (from some nanometers to some hundreds of nanometers) in which, although the deformation and crack-propagation mechanisms can be active, important differences as compared with the same mechanisms occurring at larger scales can occur. These differences can be caused by surface-topography-related factors, changes in the structure and chemical composition of the material on approaching the surface and intrinsic effects related with increasing surface to volume ratio (surface free energy, strain gradient plasticity phenomena). What happens in this poorly known transition region from bulk wear to atomic wear is still far from being understood. Certainly, in the near future, experimental results, MD simulations and the development of scale-dependent plasticity theories will bring new insights to this topic, reducing the gap between the comprehension of macro-, micro- and nanowear mechanisms.

Acknowledgement. The author would like to thank S. Graça, M. A. Fortes and M. D'Acunto for the useful discussions and suggestions, and R. Vilar for creating the conditions that result in this work. The author also thanks the Portuguese Foundation for Science and Technology (FCT – Project Nanonico, POCTI/CTM/59376/2004), and also the European Science Foundation (ESF) scientific program "NATRIBO", for the financial support of the nanotribology research line at IST.

References

1. H.P. Jost, Lubrication (tribology) - A report of the present position and industry's needs, Dept. of Science and Education, H. M. Stationery Office, London, U.K. (1966).
2. H.P. Jost, Economic impact of tribology, Mechanical Engineering, August, 26–33 (1975).

3. E. Rabinowicz, Friction and Wear of Materials. 2nd edn, John Wiley and Sons (1995).
4. H. Liu and B. Bhushan, Nanotribological characterization of digital micromirror devices using an atomic force microscope, Ultramicroscopy, 100, 391–412 (2004).
5. S.S. Perry and W.T. Tysoe, Frontiers of fundamental tribological research, Tribology Letters, 19 (3), 151–161 (2005).
6. R. Colaço and R. Vilar, A model for the abrasive wear of metallic matrix particle-reinforced materials, Wear, 254 (7–8), 625–634 (2003).
7. A Strategy for Tribology in Canada, National Research Council of Canada, Canada (1986).
8. An investigation on the application of tribology in China, Tribology Institute of the Chinese Mechanical Engineering Society, China (1986).
9. J. Krim, Surface science and the atomic scale origins of friction: what once was old is new again, Surface Science, 500, 741–758 (2002).
10. J.B. Adams, L.G. Hector, D.J. Siegel, H. Yu and J. Zhong, Adhesion, lubrication and wear on the atomic scale, Surface and Interface Analysis, 31, 619–626 (2001).
11. I.M. Hutchings, Tribology: friction and wear of engineering materials, Edward Arnold (1992).
12. B. Bushan, An introduction to tribology, John Wiley and Sons, Inc. (2002).
13. J.A. Greenwood and J.B. Williamson, Contact of nominally flat surfaces, Proceedings of the Royal Society of London, A295, 300–319 (1966).
14. G. Binnig, C.F. Quate and C. Gerber, Atomic Force Microscope, Physical Review Letters, 56 (9), 930–933 (1986).
15. S. Sundararajan and B. Bhushan, Micro/nanotribology of ultra-thin hard amorphous carbon coatings using atomic force friction force microscopy, Wear, 225–229, 678–689 (1999).
16. B. Bhushan, Nano to microscale wear and mechanical characterization using scanning probe microscopy, Wear, 251, 1105–1123 (2001).
17. R. Kaneko, K. Nonaka and K. Yasuda, Scanning Tunneling Microscopy and Atomic Force Microscopy for Nanotribology, Journal of Vacuum Science & Technology A - vacuum surfaces and films, 6 (2), 291–292 (1988).
18. Z. Jiang, C.-J. Lu, D.B. Bogy and T. Miyamoto, An investigation of the experimental conditions and characteristics of a nanowear test, Wear, 181–183 777–783 (1995).
19. S. Miyake, T. Miyamoto and R. Kaneko, Increase of nanometer-scale wear of polished chemical-vapor-deposited diamond films due to nitrogen ion implantation, Nuclear Instruments and Methods in Physics Research B - beam interactions with materials & atoms, 108, 70–74 (1996).
20. K.-H. Chung, Y.-H. Lee, D.-E. Kim, J. Yoo and S. Hong, Tribological characteristics of probe tip and PZT media for AFM-based recording technology, IEEE Transactions on Magnetics, 41 (2), 849–854 (2005).
21. S. Graça, R. Colaço and R. Vilar, Using atomic force microscopy to retrieve nanomechanical surface properties of materials, Materials Science Forum, 514–516, 1598–1602 (2006).
22. A.R. Machcha, M.H. Azarian and F.E. Talke, An investigation of nano-wear during contact recording, Wear, 197, 211–220 (1996).
23. E. Gnecco, R. Bennewitz and E. Meyer, Abrasive wear on the atomic scale, Physical Review Letters, 88 (21), 215501/1–215501/4 (2002).

24. W. Gulbinski, T. Suszko and D. Pailharey, High load AFM friction and wear experiments on V2O5 thin films, Wear, 254, 988–993 (2003).
25. J.Y. Park, D.F. Ogletree, M. Salmeron, C.J. Jenks and P.A. Thiel, Friction and adhesion properties of clean and oxidized Al-Ni-Co decagonal quasicrystals: a UHV atomic force microscopy/scanning tunneling microscopy study, Tribology Letters, 17 (3), 629–636 (2004).
26. J. Drelich, G.W. Tormoen and E.R. Beach, Determination of solid surface tension from particle-substrate pull-off forces measured with the atomic force microscope, Journal of Colloid and Interface Science, 280, 484–497 (2004).
27. H. Gao, Y. Huang, W.D. Nix and J.W. Hutchinson, Mechanism-based strain gradient plasticity-I. Theory, Journal of the Mechanics and Physics of Solids, 47, 1239–1263 (1999).
28. Y.G. Wey and J.W. Hutchinson, Steady-state crack growth and work of fracture for solids characterized by strain gradient plasticity, Journal of the Mechanics and Physics of Solids, 45 (8), 1253–1273 (1997).
29. G. Elssner, D. Korn, R.M. Cannon and M. Rühle, Fracture properties of interfacially doped Nb-Al_2O_3 bicrystals: I, fracture characteristics, Acta Materialia, 50 (15), 3881–3901 (2002).
30. K.-H. Zum Gahr, Microstructure and Wear of Materials, Elsevier Scientific Publishing Company (1987).
31. H. Luth, Surfaces and interfaces of solids, Springer-Verlag (1993).
32. F.P. Bowden, A.J.W. Moore and D. Tabor, The plowing and adhesion of sliding metals, Journal of Applied Physics, 14, 80–91 (1943).
33. G.I. Finch, A.G. Quarrekk and J.S. Roebuck, The Beilby Layer, Proc. of the Royal Society of London, 145 (855), 676–681 (1934).
34. B.W.E. Avient and H. Wilman, New features of the abrasion process shown by soft metals: the nature of mechanical polishing, British Journal of Applied Physics, 13, 521–526 (1962).
35. L.H. Gerner, Diffraction of electrons by metal surfaces, Physical Review, 43 (9), 724–726 (1933).
36. D.M. Turley and L.E. Samuels, The nature of mechanically polished surfaces of copper, Materials Characterization, 39 (2–5), 399–418 (1997).
37. K.L. Johnson, K. Kendall and D. Roberts, Surface Energy and the Contact of Elastic Solids, Proceedings of the Royal Society of London, A 324, 301–313 (1971).
38. K.N.G. Fuller and D. Tabor, The effect of surface roughness on the adhesion of elastastic solids, Proceedings of the Royal Society of London, A 345, 327–342 (1975).
39. T.R. Thomas, Rough surfaces, Longman, London and New York (1982).
40. L. Zhou, M. Beck, H. Gatzen, K. Altshuler and F. Talke, Slider vibration reduction using slider surface texture, Microsystem Technologies - micro- and nanosystems - information storage and processing systems, 11 (8–10), 857–866 (2005).
41. T. Hisakado and T. Tsukisoe, Effect of surface roughness on transient wear, Journal of the Japan Society of Lubrication Engineers, 21 (4), 228–235 (1976).
42. S. Gantiand B. Bhushan, Generalized fractal analysis and its application to engineering surfaces, Wear, 180, 17–34 (1995).
43. H.H. Gatzen and M. Beck, Wear of single crystal silicon as a function of surface roughness, Wear, 254, 907–910 (2003).

44. X. Wang, K. Kato and K. Adachi, Running-in effect on the load-carrying capacity of a water-lubricated SiC thrust bearing, Proceedings of the Institution of Mechanical Engineers Part J - Journal of Engineering Tribology, 219 ((J2)), 117–124 (2005).
45. M.A. Fortes, R. Colaço and M.F. Vaz, Contact mechanics of cellular solids, Wear, 230, 1–10 (1999).
46. D. Tabor, Lubrication and Wear, in Surface and Colloid Science, E. Matijevic, Ed. John Wiley. 245–312 (1972).
47. R. Colaço and R. Vilar, On the influence of retained austenite in the abrasive wear behavior of a laser surface melted tool steel, Wear, 258 (1–4), 225–231 (2005).
48. R. Holm, Electrical contacts, H. Gerber Pub, Stockholm (1946).
49. J.F. Archard, Contact and rubbing of flat surfaces, Journal of Applied Physics, 24 (8), 981–988 (1953).
50. D.A. Rigney, Some thoughts on sliding wear, Wear, 152 187–192 (1992).
51. D. Tabor, The hardness of metals. Oxford Classic Texts, Clarendon Press (1951).
52. E. Rabinowicz, Friction and wear of materials, John Wiley and Sons (1965).
53. A.G. Evans, Abrasive wear of ceramics, American Ceramic Society Bulletin 56 (3): 292–292 1977, 56 (3), 292–292 (1977).
54. U. Landman, W.D. Luedtke and E.M. Ringer, Atomistic mechanisms of adhesive contact formation and interfacial processes, Wear, 153 (1), 3–30 (1992).
55. J.A. Harrison, R.J. Colton, C.T. White and D.W. Brenner, Effect of atomic-scale surface roughness on friction - a molecular-dynamics study of diamond surfaces, Wear, 168 (1–2), 127–133 (1993).
56. R. Bassani and M. D'Acunto, Nanotribology: tip-sample wear under adhesive contact, Tribology international, 33, 443–452 (2000).
57. M. D'Acunto, Wear and diffusive processes, Tribology international, 36, 553–558 (2003).
58. M. D'Acunto, Theoretical approach for the quantification of wear mechanisms on the nanoscale, Nanotechnology, 15, 795–801 (2004).
59. S.C. Lim and M.F. Ashby, Wear-mechanism maps, Acta Metallurgica, 35 (1), 1–24 (1987).
60. C.L. Kelchner, S.J. Plimpton and J.C. Hamilton, Dislocation nucleation and defect structure during surface indentation, Physical Review B, 58 (17), 11085–11088 (1998).
61. J.A. Zimmerman, C.L. Kelchner, P.A. Klein, J.C. Hamilton and S.M. Foiles, Surface step effects on nanoindentation Physical Review Letters, 87 (16), paper 165507 (2001).
62. I. Szlufarska, R.K. Kalia, A. Nakano and P. Vashishta, Atomistic mechanisms of amorphization during nanoindentation of SiC: A molecular dynamics study, Physical Review B, 71 (17), paper 174113 (2005).
63. E.T. Lilleodden, J.A. Zimmerman, S.M. Foiles and W.D. Nix, Atomistic simulations of elastic deformation and dislocation nucleation during nanoindentation, Journal of the Mechanics and Physics of Solids, 51 (5), 901–920 (2003).
64. N.A. Fleck and J.W. Hutchinson, A phenomenological theory to for strain gradient effects in plasticity, Journal of the Mechanics and Physics of Solids, 41 (12), 1825–1857 (1993).

65. K.W. McElhaney, J.J. Vlassak and W.D. Nix, Determination of indenter tip geometry and indentation contact area for depth-sensing indentation experiments, Journal of Materials Research, 13 (5), 1300–1306 (1998).
66. Y. Liu and A.H.W. Ngan, Depth dependence of hardness in copper single crystals measured by nanoindentation, Scripta Materialia, 44, 237–241 (2001).
67. N.A. Stelmashenko, M.G. Walls, L.M. Brown and Y.V. Milan, Microindentations on W and Mo oriented single crystals - an STM study, Acta Metallurgica et Materialia, 41 (10), 2855–2865 (1993).
68. Q. Ma and D.R. Clarke, Size dependent hardness of silver single crystals, Journal of Materials Research, 10 (4), 853–863 (1995).
69. A.A. Elmoustafa and D.S. Stone, Indentation size effect in polycrystalline FCC metals, Acta Materialia, 50 (14), 3641–3650 (2002).
70. S. Graça, R. Colaço and R. Vilar, Indentation size effect in laser clad nickel and cobalt, (to be published).
71. S.J. Bull, On the origins and mechanisms of the indentation size effect, Z. Metallkd, 94 (7), 787–792 (2003).
72. H. Li, A. Ghosh, Y.H. Han and R.C. Bradt, The frictional component of the Indentation size effect in low load microhardness testing, Journal of Materials Research, 8 (5), 1028–1032 (1993).
73. J.G. Swadener, A. Misra, R.G. Hoagland and A. Nastasi, A mechanistic description of combined hardening and size effects, Scripta Materialia, 47 (5), 343–348 (2002).
74. H. Gao and Y. Huang, Geometrically necessary dislocation and size-dependent plasticity, Scripta Materialia, 48 113–118 (2003).
75. W.D. Nix and H. Gao, Indentation size effects in crystalline materials: a law for strain gradient plasticity, Journal of Mechanics and Physics of Solids, 46 (3), 411–425 (1998).
76. T.-Y. Zhang and W.-H. Xu, Surface effects on nanoindentation, Journal of Material Research, 17 (7), 1715–1720 (2002).
77. I.L. Jager, Surface free energy - a possible source of error in nanohardness?, Surface Science, 565 (2–3), 173–179 (2004).
78. F.R.N. Nabarro and J.P. Hirth, Dislocations in solids, ed. F.R.N. Nabarro and J.P. Hirth, Vol. Volume 11, Elsevier (2002).
79. M.F. Ashby, The deformation of plastically non-homogeneous alloys, Philosphical Magazine, 21 399–424 (1970).
80. J.F. Nye, Some geometrical relations in dislocated crystals, Acta Metallurgica, 1 (2), 153–162 (1953).
81. N.A. Fleck, G.M. Muller, M.F. Ashby and J.W. Hutchinson, Strain gradient plasticity: theory and experiment, Acta Metallurgica et Materialia, 42 (2), 475–487 (1994).
82. N.A. Fleck and J.W. Hutchinson, Strain gradient plasticity, Advances in Applied Mechanics, 33 295–361 (1997).
83. R.W. Carpick and M. Salmeron, Scratching the surface: fundamental investigations of tribology with atomic force microscopy, Chemical Review, 97, 1163–1194 (1997).
84. B. Bhushan, Nanotribology and nanomechanics, Wear, 259, 1507–1531 (2005).
85. A.G. Khursudov, K. Kato and H. Koide, Wear of the AFM diamond tip sliding against silicon, Wear, 203–204, 22–27 (1997).

86. K.-H. Chung, Y.H. Lee and D.-E. Kim, Characteristics of fracture during the approach process and wear mechanism of a silicon AFM tip, Ultramicroscopy, 102, 161–171 (2005).
87. R. Lüthi, E. Meyer, H. Haefke, L. Howald, W. Gutmannsbauer, M. Guggisberg, M. Bammerlin and H.-J. Güntherodt, Nanotribology: an UHV-SFM study on thin films of C60 and AgBr, Surface Science, 338 (1–3), 247–260 (1995).
88. P.E. Sheehan, The wear kinetics of NaCl under dry nitrogen and at low humidities, Chemical Physics Letters, 410 (1–3), 151–155 (2005).
89. E. Gnecco, R. Bennewitz, A. Socoliuc and E. Meyer, Friction and wear on the atomic scale, Wear, 254, 859–862 (2003).
90. A. Socoliuc, E. Gnecco, R. Bennewitz and E. Meyer, Ripple formation induced in localized abrasion, Physical Review B, 68, paper 115416 (2003).
91. K.-H. Chung and D.-E. Kim, Fundamental investigation of micro wear rate using an atomic force microscope, Tribology Letters, 15 (2), 135–144 (2003).
92. B. Bhushan and A.V. Kulkarni, Effect of normal load on microscale friction measurements, Thin Solid Films, 278 (1–2), 49–56 (1996).
93. J. Hu, X.-D. Xiao, D.F. Ogletree and M. Salmeron, Atomic scale friction and wear of mica, Surface Science, 327 358–370 (1995).
94. S. Miyake, 1 nm deep mechanical processing of muscovite mica by atomic force microscopy, Applied Physics Letters, 67 (20), 2925–2927 (1995).
95. D.D. Woodland and W.N. Unertl, Initial wear in nanometer-scale contacts on polystyrene, Wear, 203–204, 685–691 (1997).
96. S.P. Ho, R.W. Carpick, T. Boland and M. LaBerge, Nanotribology of CoCr-UHMWPE TJR prosthesis using atomic force microscopy, Wear, 253, 1145–1155 (2002).
97. J.S.S. Wong, H.-J. Sue, K.-Y. Zeng, R.K.Y. Li and Y.-W. Mai, Scratch damage of polymers in nanoscale, Acta Materialia, 52 (2), 431–443 (2004).
98. Z.G. Jiang, C.J. Lu, D.B. Bogy and T. Miyamoto, An investigation of the experimental conditions and characteristics of a nano-wear test, Wear, 181, 777–783 (1995).
99. Z.G. Jiang, C.J. Lu, D.B. Bogy and T. Miyamoto, Dependence of nano-friction and nano-wear on loading force for sharp diamond tips sliding on Si, Mn-Zn ferrite and Au, Journal of Tribology - Transactions of the ASME, 117 (2), 328–333 (1995).
100. W. Lu and K. Komvopoulos, Nanomechanical and nanotribological properties of carbon, chromium, and titanium carbide ultrathin films, Journal of Tribology - Transactions of the ASME, 123 (4), 717–724 (2001).
101. J.M. Helt and J.D. Batteas, Wear of mica under aqueous environments: direct observation of defect nucleation by AFM, Langmuir, 21, 633–639 (2005).
102. D.F. Wang and K. Kato, Nano-scale fatigue wear of carbon nitride coatings: part I-wear properties, Journal of Tribology: Transactions of the ASME, 125 430–436 (2003).
103. D.F. Wang and K. Kato, Nano-scale fatigue wear of carbon nitride coatings: part II-wear mechanisms, Journal of Tribology - Transactions of the ASME, 125 437–444 (2003).
104. U. Beerschwinger, T. Albrecht, D. Mathieson, R.L. Reuben, S.J. Yang and M. Taghizadeh, Wear at microscope scales and light loads for MEMS applications, Wear, 181 426–435 (1995).

105. S. Sundararajan and B. Bhushan, Micro/nanotribological studies of polysilicon and SiC films for MEMS applications, Wear, 217 251–261 (1998).
106. A.R. Krauss, O. Auciello, D.M. Gruen, A. Jayatissa, A. Sumant, J. Tucek, D.C. Mancini, N. Moldovan, A. Erdemir, D. Ersoy, M.N. Gardos, H.G. Busmann, E.M. Meyer, M.Q. Ding, Ultrananocrystalline diamond thin films for MEMS and moving mechanical assembly devices, Diamond and Related Materials, 10 (11), 1952–1961 (2001).